



Investigation of the droplet characteristics and size distribution during the collaborative atomization process of a twin-fluid nozzle

Bo Chen^{1,2} · Dianrong Gao³ · Yanbiao Li¹ · Chaoqun Chen¹ · Xiaoming Yuan^{2,3} · Zesheng Wang¹ · Peng Sun¹

Received: 29 October 2019 / Accepted: 23 February 2020 / Published online: 4 March 2020
© Springer-Verlag London Ltd., part of Springer Nature 2020

Abstract

To overcome the environmental problems during manufacturing process, the twin-fluid atomization has been demonstrated as an efficient technique to reduce the lubri-cooling fluid consumption and its pollution emission. However, the coupling between the gas, liquid, and structure of the twin-fluid nozzle directly affect the droplet characteristics and size distribution, which has a significant effect on the processing performance. In the current work, the droplet characteristics during the collaborative atomization process of a twin-fluid nozzle with two kinds of atomizing cores are investigated and compared via a phase Doppler particle analyzer (PDPA), and the droplet diameter and size distribution of a new twin-fluid nozzle (NTN) with different atomizing cores are further investigated. The results reveal that the spray atomization characteristics and droplet size distribution are obviously influenced by the performance of primary and secondary atomization, which mainly depend on the atomizing core structure and the gas to liquid mass flow rate ratio (GLR). Because the gas acceleration performance of the new atomizing core is better than that of the standard atomizing core at the same GLR, compared with the standard twin-fluid nozzle (STN), the droplet diameter decreases by approximately 33.97%, the droplet number concentration and axial velocity increase by approximately 36.39% and 34.51%, respectively, and the spray cone angle of the STN is only approximately 80% of that of the NTN. Meanwhile, the higher GLR of the twin-fluid nozzle provides more energy for the droplets, so the viscous force between the liquids is easier to overcome and the atomization characteristics are improved. Nevertheless, for a smaller GLR, the droplet size distribution is significantly affected by the structural parameters of the NTN atomizing core due to the insufficient atomization power. Moreover, a smaller throat diameter, a smaller exit diameter, and a moderate distance between the liquid channel and the atomizing core exit are beneficial for improving the droplet cumulative distribution.

Keywords Collaborative atomization · GLR · Twin-fluid nozzle · Droplet diameter · Size distribution

1 Introduction

In recent years, an increase in environmental pollution caused by the rapid industrialization is obvious, and it has attracted

widespread attention. In the manufacturing process, the importance of environmental protection is increasingly recognized. The liquid used for lubrication and cooling during processing has an important influence on the tool life and the surface quality, and the reduction of liquid consumption and pollution emission is of great significance. To solve this problem, the use of atomization to break a continuous liquid into discrete droplets has proven to be an effective method [1]. Spray atomization can be used for minimum quantity lubrication (MQL), cooling, and chemical mechanical polishing. Indeed, the spray atomization performance, such as the droplet characteristics and size distribution, is directly related to the lubrication performance, the heat exchange capability, and the surface quality [2–4]. In spray atomization technologies, the use of the twin-fluid atomization technology to improve the spray performance has been proven to be an efficient approach [5, 6], and the main principle of small droplet formation in this

✉ Yanbiao Li
liybjut@163.com

¹ Key Laboratory of E & M, Ministry of Education & Zhejiang Province, Zhejiang University of Technology, Hangzhou 310032, China

² State Key Laboratory of Fluid Power and Mechatronic Systems, Zhejiang University, Hangzhou 310027, China

³ School of Mechanical Engineering, Yanshan University, Qinhuangdao 066004, China

technique is that the liquid sheet is disrupted into droplets by the energy of the high-velocity pressurized gas. This technique has the advantages of smaller droplet size, lower cost, and higher operating reliability and has received extensive attention from scholars worldwide [7, 8].

Due to the strong coupling between the gas, liquid, and mechanical structure, the spray process of twin-fluid atomization is complex and changeable. Some deficiencies, such as low droplet concentration, uneven size distribution, and poor atomization stability, still exist in practical applications. Therefore, to improve the droplet characteristics of twin-fluid atomization, a thorough understanding of the method and behavior of twin-fluid atomization is significant. Many investigations on atomization methods have been reported to improve the droplet characteristics of twin-fluid atomization, which can be achieved by different approaches, including electrostatic, supersonic, and vibrating techniques [9–11]. These methods have the advantages of simple operating conditions, high efficiency, and strong adaptability, which have attracted the interest of researchers.

Various studies of spray nozzles related to vibrating atomization have been previously performed using numerical and experimental methods. Kim and Choi [12] numerically analyzed the atomization of an ultrasonic gas nozzle with computational fluid dynamics (CFD). At the same time, the ultrasonic vibration generated by the resonance chamber in the gas nozzle was decided by the experiment. Baillot et al. [13] investigated the influence of transverse acoustic perturbations on a coaxial air-assisted nozzle through a comparative experiment. This study verified that the breakup of the liquid sheet was mainly affected by the membrane breakup, faraday instability, and intrinsic sheet instabilities, which are closely related to the acoustics. Narayanan [14, 15] proposed a novel atomization nozzle based on the Hartmann effect, and the influence of Hartmann cavity acoustics on spray atomization was experimentally investigated. The results showed that the acoustic field could enhance the atomization behavior and caused the droplet to undergo large deformations, resulting in an irregular shape. Ruan et al. [16] designed a vibrating atomization nozzle and experimentally studied the acoustic field characteristics, and the effect of the acoustic field on droplet deformation behavior was further investigated. The results revealed that the atomization quality could be improved by the droplet oscillation greatly enhanced by the acoustic field. Ficuciello et al. [17] experimentally investigated the effect of a high-amplitude transverse acoustic field on the spray atomization of a coaxial atomizing nozzle, and the drastic effect of the acoustics on the atomization process was verified. Vibrating atomization technology can significantly improve the atomization performance, but the reduction in droplet size and the increase in droplet concentration are limited, and the droplet characteristics have yet to be further improved.

An increase in the velocity difference between gas and liquid two phases was proven to be an effective method to

promote the droplet characteristics, and a supersonic atomization method to increase the overall atomization performance by accelerating the airflow velocity to supersonic speeds to enhance the droplet breakup was proposed by Gelfand [18]. Theofanous [19] suggested that accelerating the gas speed from low subsonic to supersonic to increase the mode competition between Rayleigh–Taylor and Kelvin–Helmholtz instabilities could enhance the droplet breakup and the atomization performance. Yang et al. [20] analyzed the velocity flow field distributions inside a supersonic atomizing nozzle, and the influence of the operational parameters on the atomization performance was further studied. The results indicated that the increase in gas pressure and decrease in liquid pressure was beneficial for decreasing the droplet size. Mates and Settles [21, 22] investigated the gas dynamics and atomization behavior of an atomizing nozzle during the fine metal powder atomization process, and the potential to remarkably improve particle size control and energy efficiency was verified. Furthermore, the results indicate that the supersonic gas flow could provide more energy to enhance the multistage droplet breakup, and the particle size was obviously influenced by the velocity decay. However, a collaborative atomization method for improving the droplet characteristics based on supersonic atomization technology and vibrating atomization technology has rarely been reported to date, and the droplet characteristics, droplet diameter, and size distribution during the collaborative atomization process have not been previously studied in detail.

During the manufacturing processes, better droplet characteristics and size distribution of the atomization nozzle can effectively enhance the capillary penetration performance and heat transfer property, which is of great significance for improving the tool life and surface quality [1, 3, 4]. Thus, in order to improve the droplet characteristics and size distribution of the twin-fluid atomizing nozzle during the lubrication, based on the previous work of Chen et al. [23, 24], the collaborative atomization method was adopted and a new twin-fluid nozzle was designed. The quantitative measurements of the droplet characteristics of twin-fluid nozzle were conducted by a phase Doppler particle analyzer. The spray atomization characteristics of the twin-fluid nozzle with two kinds of atomizing cores were investigated and compared, and the droplet diameter and size distribution of a new twin-fluid nozzle with different atomizing cores were further analyzed during collaborative atomization.

2 Experimental description

2.1 Experimental setup

Figure 1 shows the schematic of a twin-fluid atomization experimental setup designed to perform the spray atomization

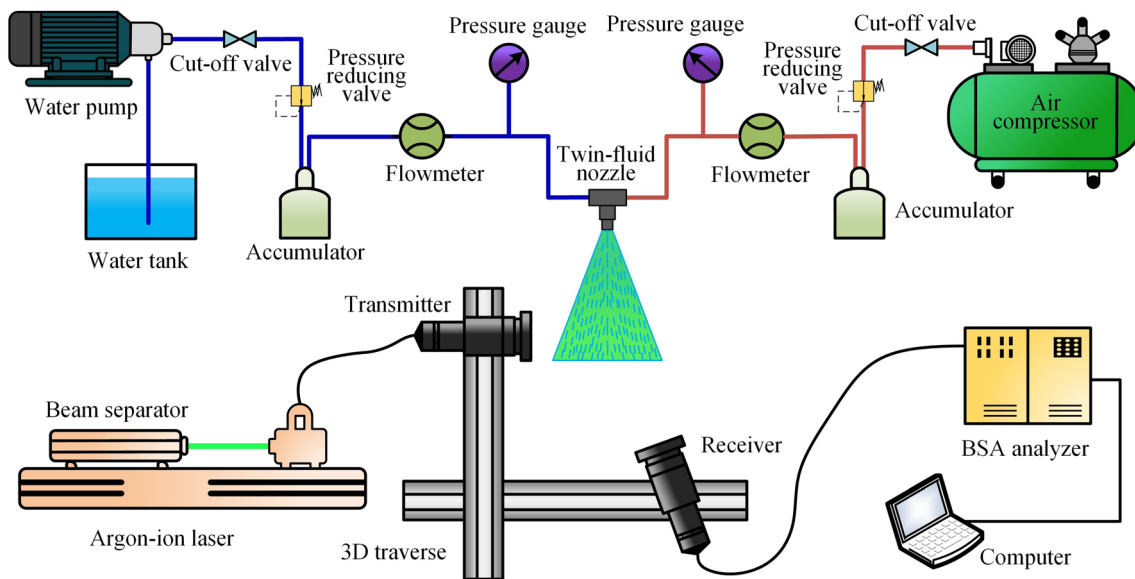


Fig. 1 Schematic of the twin-fluid atomization experimental setup

experiment. The experimental setup is mainly composed of a twin-fluid nozzle, a water pump, an air compressor, two flowmeters, two accumulators, two pressure reducing valves, two cut-off valves, two pressure gauges, and the measurement system. Liquid and gas are pumped into the setup by the water pump and air compressor, respectively, and the pressure in the pipelines can be adjusted by the pressure reducing valve to the specified values to meet the experimental requirements. In the pipelines, the fluctuations in the working fluids can be absorbed, the pressures can be stabilized through the accumulator, and the values of the pressure and the flow rate can be measured by a pressure gauge and a flowmeter, respectively. The liquid and gas in the pipes are injected into the twin-fluid nozzle, which is employed to achieve the atomization behavior. The measurement system is adopted to collect a sample of droplets and to obtain the droplet concentration, size, and velocity at a downstream location of the nozzle outlet.

2.2 Testing nozzle

A schematic of the twin-fluid nozzle used in this study is shown in Fig. 2. The nozzle has a nozzle shell with an atomizing core contained within the shell. A self-excited vibrating cavity is located near the downstream of the nozzle outlet and is fixed to the nozzle shell. The length and maximum outer diameter of the atomizing core are 9.5 mm and 8 mm, respectively, and it has 4 circumferentially evenly distributed liquid channels with a diameter of 0.9 mm. Liquid and gas flow into the atomizing core through the liquid inlet and gas inlet, respectively, and the complex coupling behavior of gas-liquid mixing and liquid film breakup occur inside the atomizing core. Atomized droplets spray from the nozzle outlet at high speed and strongly drive the self-excited vibrating cavity, which causes a high-frequency vibration of the self-excited

vibrating cavity. The excessive vibration further enhances the turbulence around the nozzle outlet, which causes the secondary atomization of the droplets. The collaborative effect of the two atomization processes can greatly improve the droplet breakup performance, and the droplets move downstream of the nozzle outlet and gradually develop a conical spray.

For the two-phase gas-liquid flow inside the twin-fluid nozzle, the atomizing core is the key component of the initial atomization. Based on the supersonic principle of the Laval effect [25, 26], the design of a new atomizing core was proposed. The structure of the gas channel of the new atomizing core mainly included a convergent section, a throat, and a divergent section. The bicubic curve equation and the arc plus line method were used for designing the convergent section and divergent section, respectively. The new atomizing core is optimized on the basis of a standard atomizing core [27], and the two types of atomizing cores with different internal structures are shown in Fig. 3. The influence of the two structures

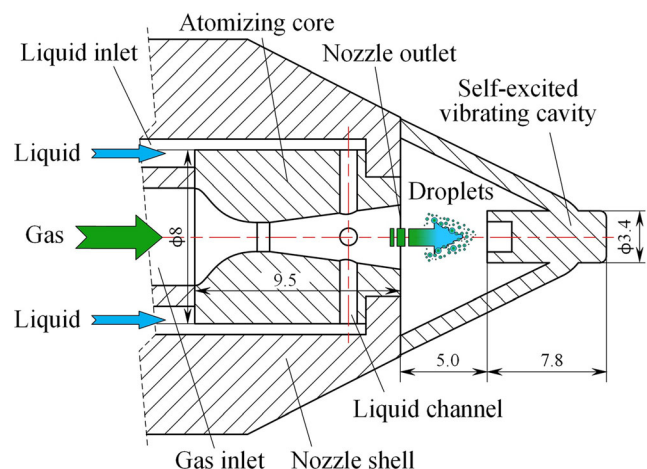


Fig. 2 Schematic of the twin-fluid nozzle geometry

on the gas flow is quite different, and the gas flow inside the new atomizing core can be quickly accelerated up to the supersonic speed by the Laval effect [28]. Four representative values of the three key geometrical parameters of the new atomizing core are further investigated. These parameters, as listed in Table 1, include the following: D_0 is the throat diameter of the new atomizing core, D_1 is the exit diameter of the new atomizing core, and L is the distance between the central axis of the liquid channel and the atomizing core exit (nozzle outlet).

2.3 Experimental conditions and measurement technique

A standard twin-fluid nozzle (STN) (twin-fluid nozzle with standard atomizing core), a new twin-fluid nozzle (NTN) (twin-fluid nozzle with new atomizing core), and various NTNs with different structures of new atomizing core were used for the atomization experiments. Each of the experimental cases was conducted with air and water as the working fluids at an ambient room temperature of 24 °C and atmospheric pressure. The detailed conditions of these experimental cases are summarized in Table 2.

To obtain the size distribution, axial velocity, and concentration of the atomized droplets, a phase Doppler particle analyzer (PDPA, Dantec Dynamics Co., Denmark) was adopted. As shown in Fig. 1, the PDPA consists of a water-cooled argon-ion laser, a 3D traverse system, a transmitter, a receiver, a beam separator, a P600 BSA analyzer, and a computer. A 6 W argon-ion laser provided the dual-channel optical fiber assembly, which transmitted two pairs of beams (514.5 nm wavelength green beam and 488 nm wavelength blue beam) by a beam separator and a frequency module for measuring the droplet properties. Both the transmitter and the receiver were equipped with front lenses with a 310 mm focal length. The receiver was positioned in a 30° forward scattering configuration, and the beam waist was approximately 85 μm in diameter at the

Table 1 Geometrical parameters of the new atomizing core

Item	Value	Range
Throat diameter D_0 (mm)	1.4	1.2, 1.4, 1.6, 1.8
Exit diameter D_1 (mm)	3.0	2.7, 3.0, 3.3, 3.6
Distance L (mm)	3.0	2.4, 3.0, 3.6, 4.2

measurement position. More details regarding the PDPA are presented in Table 3.

Each droplet moving through the small measurement volume of the intersection of two focused laser beams could be detected, and the measurement volume could be adjusted by the 3D traverse system. The evaluation of raw PDPA data was performed in post-processing mode using the BSA analyzer and was statistically analyzed via BSA Flow software. Due to the internal probe volume correction function in the software, the lower visibility of small droplets was corrected at the edge of the measurement volume. In this study, the PDPA setup was optimized for droplet diameters below 100 μm and velocities less than 50 m/s, and real-time droplet measurements were performed with a high precision of 0.2%. Settings of the PDPA in all tests were kept constant to minimize any bias in the measurement of droplet properties. For each measurement position, three replicate experiments were performed, and effective average data were obtained to ensure reliable and accurate statistical analysis.

3 Results

3.1 Comparative analysis of the effect of the atomizing core structure on the spray atomization characteristics

To investigate the variation in the spray atomization characteristics as a function of the atomizing core structure, comparative atomization experiments of the STN and NTN were

Fig. 3 Two types of atomizing cores with different internal structures. **a** Standard and **b** new

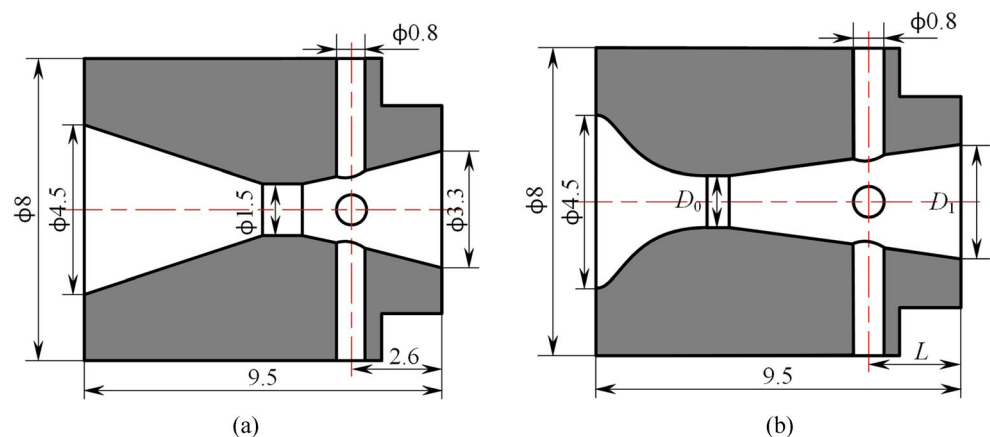


Table 2 Detailed conditions of the experimental cases

Item	Value
Room temperature (°C)	24
Atmospheric pressure (kPa)	102.6
Water density (kg·m ⁻³)	997.3
Water surface tension (N/m)	0.0721
Water viscosity (Pa·s)	0.9142 × 10 ⁻³

conducted. The studies were performed at a mass flow rate of gas from 0.00016 to 0.00034 (kg/s) and a constant liquid mass flow of 0.008 (kg/s). These values corresponded to the values of the gas to liquid mass flow rate ratio (GLR) from 2.0 to 4.3%, as shown in Table 4. From the 100 mm at the downstream location of the nozzle outlet in axial direction along the central axis of the spray, 9 measurement points with spacing of 50 mm were selected for data collection.

3.1.1 Droplet diameter

Droplets along the spray axis were measured, and the Sauter mean diameter (SMD) for various GLR values (2.0%, 2.6%, 3.3%, 3.8%, and 4.3%) of the STN and NTN are illustrated in Fig. 4. The SMD is a key criterion for atomization behavior and is calculated as follows [29]:

$$SMD = \frac{\sum_i n_i d_i^3}{\sum_i n_i d_i^2} \tag{6}$$

where d_i is the diameter of droplet i and n_i is the number of droplets.

As shown in Fig. 4 a and b, for both the sprays of the STN and NTN, the experimental data show that the SMD decreases with an increase in the GLR at a fixed liquid mass flow rate of 0.008 kg/s. The effect is in accordance with the results reported by Kourmatzis et al. [30] and Xia et al. [31]. As the GLR changes from 2.0 to 4.3%, the decrease in the SMD of the STN is more obviously affected by the increase in the GLR

Table 3 Settings and parameters of the PDPA

Parameter settings	Beam	
	Green	Blue
Beam spacing (mm)	38	38
Beam diameter (mm)	1.35	1.35
Beam half angle (°)	2.176	2.176
Bragg cell frequency (MHz)	40	40
Fringe spacing (μm)	6.775	6.426
Fringe number	35	35
Fringe direction	Negative	Negative
Scattering mechanism	Refraction	Refraction

than that of the NTN, but the overall droplet diameter of the NTN is smaller (approximately 33.97%) than that of the STN. In accordance with previous research, larger droplets more easily break up by the effect of gas injection power and surrounding turbulence [32]. However, due to the better gas acceleration performance of the NTN by the Laval effect of the new atomizing core, the higher gas velocity of the injection is beneficial for the breakup of the droplets, which results in a smaller overall droplet size. Furthermore, at a fixed water mass flow rate, the atomization power of the droplets increases with an increase in the GLR, which causes a remarkable change in the larger droplet size of the STN with the change in the GLR.

Additionally, as the droplets move during their far-field dispersion in the airflow, the SMD for each GLR increases rapidly within 400 mm of the nozzle outlet, and thereafter, with a further increase in the distance from the nozzle outlet, the increase in the SMD is weaker. The analysis of the curves demonstrates that different-sized droplets continuously coalesce during their movement, but the effect of the coalescence between the droplets gradually decreases because of the decay of droplet movement caused by the drag from the droplets and surrounding air. Thus, the droplet SMD slightly increases beyond 400 mm downstream of the spray.

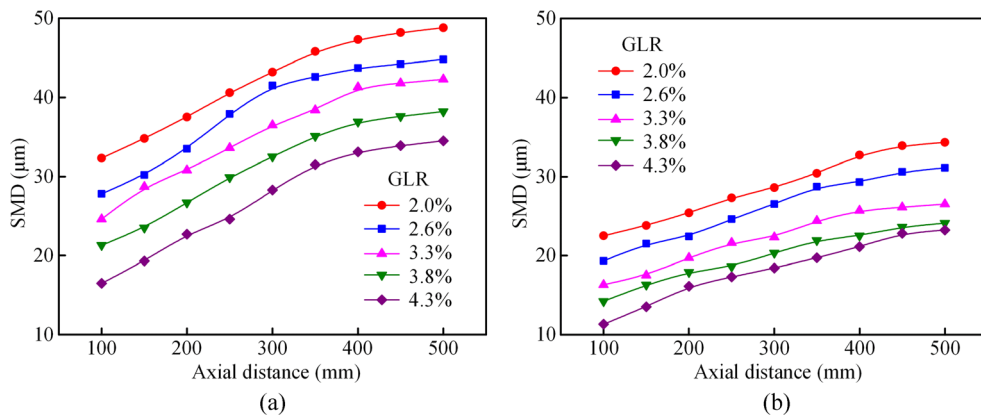
3.1.2 Droplet number concentration

The effect of various GLR values on the droplet number concentration of the STN and NTN are presented in Fig. 5. The concentration of droplets is directly related to the droplet breakup level and can be used as an important index of atomization performance [33, 34]. As seen in Fig. 5 a and b, for each GLR, the droplet number concentration presents an obvious decrease as the axial distance increases. The main reasons might be that (1) during the movement of droplets, the evaporation caused by the frictional heat generated by the surrounding air and the condensation between the droplets leading to the droplet number gradually decrease and (2) the continuous collision and aggregation between the small droplets lead to an increase in the droplet mass, which causes a falling of the larger droplets from the air. Hence, the droplet number concentration decreases as the droplets move in the air.

Table 4 Various GLR values for the atomization experiments

	Gas flow rate (kg/s)	Liquid flow rate (kg/s)	GLR (%)
1	0.00016	0.008	2.0
2	0.00021	0.008	2.6
3	0.00026	0.008	3.3
4	0.00030	0.008	3.8
5	0.00034	0.008	4.3

Fig. 4 Droplet SMD of a twin-fluid nozzle at various GLR values. **a** STN and **b** NTN



For both the STN and NTN, an obvious increase in the droplet number concentration is presented with the increase in the GLR at a fixed liquid mass flow rate. This result reveals that a higher gas mass flow rate can provide more energy, which is helpful for overcoming the viscous force between molecules inside the large droplet. Thus, the large droplet could be easily broken into smaller droplets. Meanwhile, under identical experimental conditions, the overall droplet number concentration of the NTN is higher (approximately 36.39%) than that of STN. In addition, the increase in the droplet number concentration of the NTN is remarkably affected by the increase in the GLR (2.0% to 4.3%) compared with that of the STN. Due to the better gas acceleration performance of the NTN as analyzed above, more atomizing power can be obtained, and more energy for the breakup of droplets can be provided. Hence, for the NTN, the effect of droplet breakup is more significant, and the droplet number concentration is higher.

3.1.3 Droplet axial velocity

Figure 6 illustrates the effect of the GLR (2.0%, 2.6%, 3.3%, 3.8%, and 4.3%) on the droplet mean axial velocity of the STN and NTN. For both twin-fluid nozzles, the droplet axial velocity is below 10 m/s when the axial distance is larger than 100 mm. Although the internal airflow velocity of the

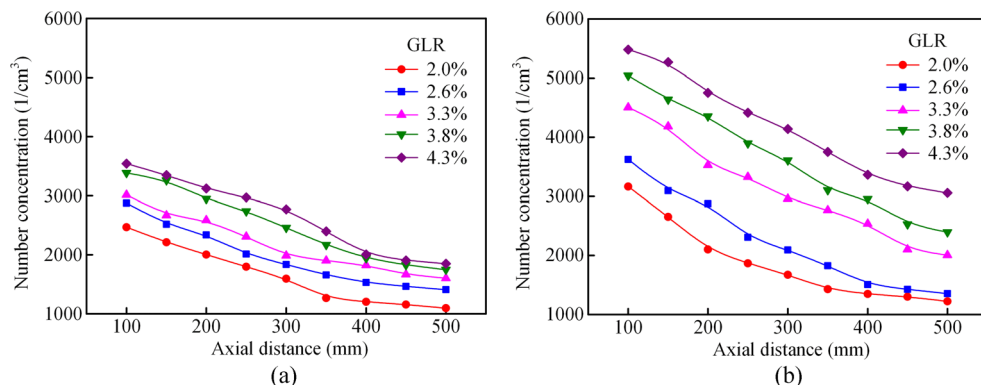
atomizing core can accelerate up to 340 m/s [20], the droplet axial velocity in the atomizing flow field decreases drastically due to the obstacle of the self-excited vibrating cavity and the strong turbulence of the secondary atomization around the nozzle outlet. Moreover, Fig. 6 a and b clearly show that the droplet axial velocity obviously decreases as the axial distance increases, and the main reason is the decay of droplet momentum, which is mainly caused by the friction from the surroundings and the adhesion between the droplets.

Furthermore, as shown in Fig. 6 a and b, at a fixed liquid mass flow rate of 0.008 kg/s, the droplet axial velocity clearly increases with an increase in the GLR of the STN and NTN. That is, an increase in gas mass flow rate significantly affects the increase in the droplet axial velocity. A noteworthy point of the two twin-fluid nozzles is ascertained when comparing the variation trend of each GLR, i.e., the values of the overall droplet axial velocity of the NTN are larger (approximately 34.51%) than that of the STN. This phenomenon is a result of the increase in the injection power that is caused by the acceleration effect of the new atomizing core.

3.1.4 Spray cone angle

The spray cone angle of the STN and NTN under various conditions was measured and investigated as specified in Table 4. The conditional spray cone angle was adopted and

Fig. 5 Droplet number concentration of a twin-fluid nozzle at various GLR values. **a** STN and **b** NTN



a detailed description of the definition and measurement method is available in previous studies [24, 35]. As shown in Fig. 7, the spray cone angle of the STN is approximately 80% of that of the NTN. Due to the obstacle of the self-excited vibrating cavity at the downstream location of the nozzle outlet, the spray along the axial direction is partly resisted, and droplets diffuse radially after they impact the self-excited vibrating cavity. If the droplets have a large velocity, then the radial component of the velocity is larger when they diffuse radially. Therefore, the spray cone angle of the NTN is larger than that of the STN, which is a result of the larger droplet velocity sprayed by the NTN.

Furthermore, with an increase in the GLR at a fixed liquid mass flow rate, the spray cone angle shows a significant increase for both twin-fluid nozzles. As discussed above, the higher GLR can provide stronger atomization energy, which is helpful for obtaining more small droplets and increasing the radial component of the droplet velocity. Smaller droplets more easily change their original trajectory under the effect of a higher injection power, which means that a higher GLR value will lead to a larger spray cone angle of the twin-fluid nozzle.

3.2 Effect of the atomizing core structure on the droplet size distribution characteristics

As discussed in Section 3.1, the atomizing core is a key component of the twin-fluid nozzle, which atomizes the two-phase fluid into droplets and plays a significant role in improving atomization performance. However, the droplet size distribution characteristics are an important index for evaluating the breakup of droplets, and the excellent droplet size distribution characteristics are helpful for improving the overall spray atomization behavior. In this section, the NTN with a new atomizing core was selected because of its better spray atomization characteristics, and experimental investigations were conducted to further illustrate the effect of the atomizing core structure on the droplet size distribution characteristics. Under various GLR values (2.0%, 2.6%, 3.3%, 3.8%, and 4.3%), the

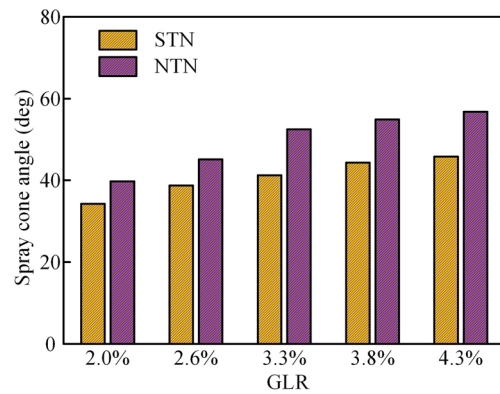


Fig. 7 Spray cone angle of a twin-fluid nozzle at various GLR values

data at measurement points 50 mm away from the nozzle outlet along the central axis of the spray in the atomizing flow field were collected, and the percent and cumulative distribution of the droplet diameters for different atomizing core structures were assessed.

3.2.1 Effect of the throat diameter on the droplet size distribution characteristics

The droplet diameter of the NTN at various GLR values was measured, and the variation in the droplet counts percent as a function of different throat diameters of the atomizing core ($D_1 = 3.0$ mm, $L = 3.0$ mm) is presented in Fig. 8. The curve of the log-normal distribution is obtained by modifying the droplet size distribution after atomization using the log-normal method [36]. When the GLR increases from 2.0 to 4.3%, the peak of the droplet size distribution moves to the left. The result reveals that the overall droplet size is smaller and more concentrated with an increase in GLR, and a larger GLR is helpful for improving the droplet size distribution characteristics. The increase in the GLR leads to an increase in atomizing power as mentioned above, which provides the droplets with more energy, and the breakup of droplets becomes easier. The droplet size decreases rapidly as the larger droplet breaks into a smaller droplet, and the further breakup

Fig. 6 Droplet axial velocity of a twin-fluid nozzle at various GLR values. a STN and b NTN

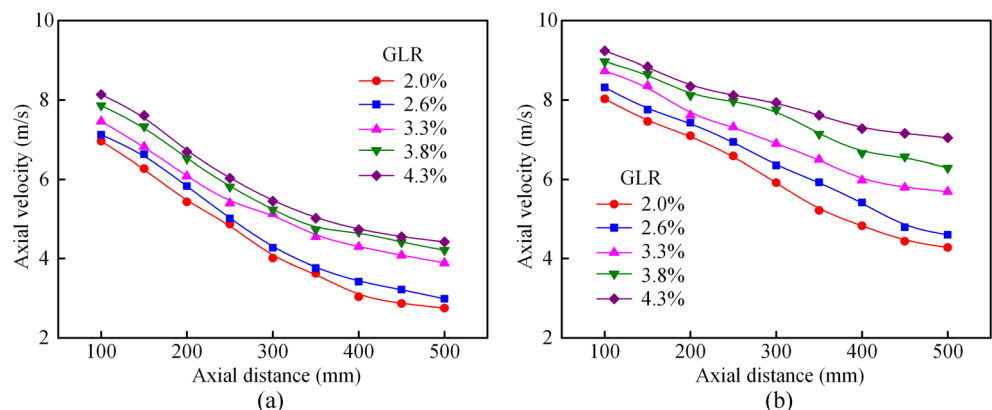
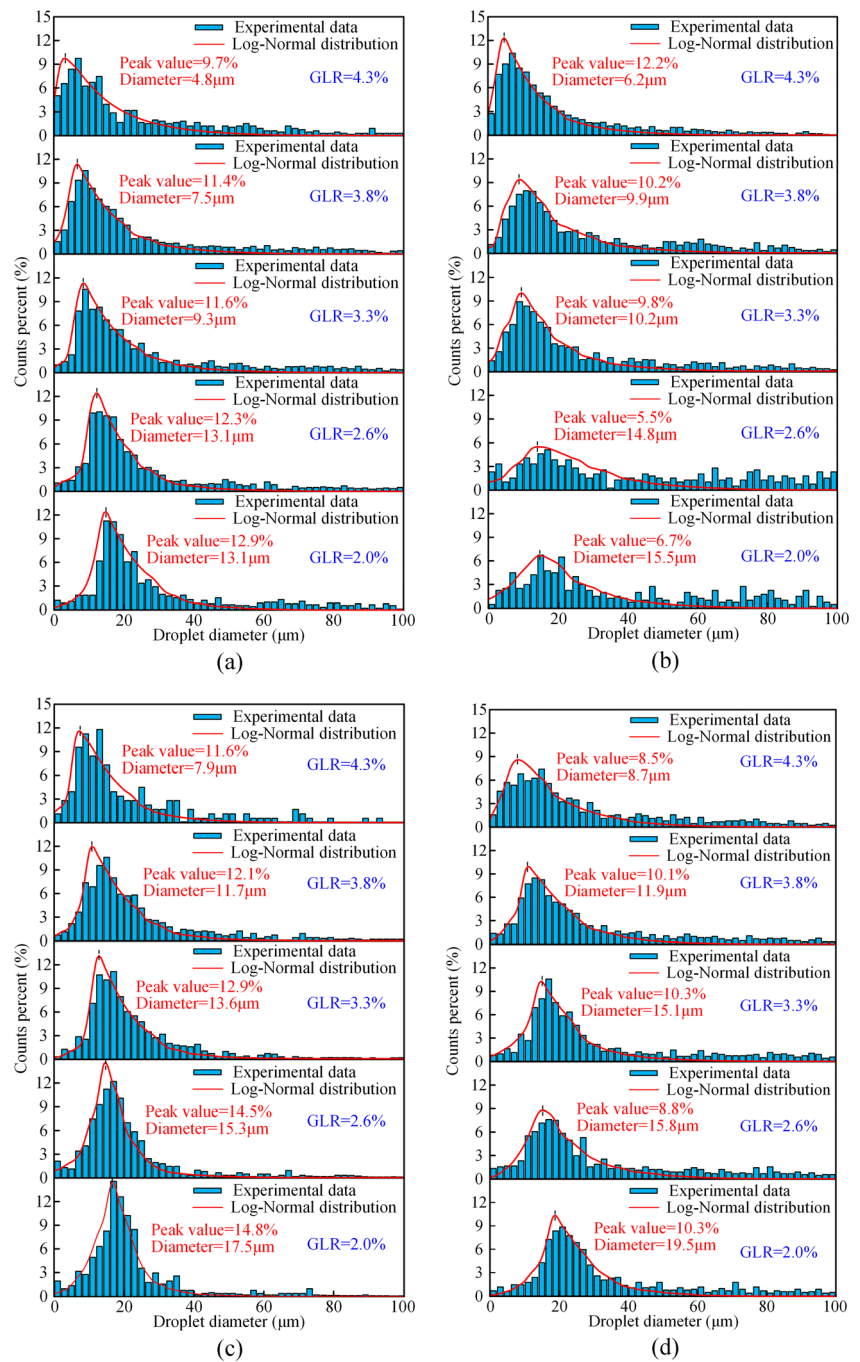


Fig. 8 Influence of the throat diameter of the atomizing core on the droplet counts percent at various GLR values.
a $D_0 = 1.2$ mm. **b** $D_0 = 1.4$ mm.
c $D_0 = 1.6$ mm and **d** $D_0 = 1.8$ mm



of the droplet becomes difficult as the droplet size decreases. Thus, the difference in the droplet size is reduced.

Furthermore, under the same GLR (such as a GLR of 4.3%), for $D_0 = 1.2$ mm, the peak appears at $4.8 \mu\text{m}$ with a value of 9.7%. However, the peak and counts percent of the droplet size distribution are $8.7 \mu\text{m}$ and 8.5% for $D_0 = 1.8$ mm, respectively. The peak of the droplet size distribution shows an increasing trend as the throat diameter of the atomizing core increases, and the ratio of the small droplet decreases, while that of the large droplet increases. This result indicates that the increase in the throat diameter is not

beneficial for improving the atomization performance. Due to the decrease in the gas velocity caused by the increase in the throat diameter, the atomization energy decreases, and the performance of primary and secondary atomization declines, which leads to a difficulty in the droplet breakup. This result is consistent with similar investigations, which reveals that a decrease in the gas velocity inside and outside the nozzle is caused by an increase in the throat diameter [20].

The influence of the throat diameter of the atomizing core on the droplet cumulative distribution at various GLR values is illustrated in Fig. 9. As the scale of the cumulative

distribution and droplet diameter are in the range of 0–100% and 0–100 μm, respectively, a dashed diagonal line is added in these four figures, which means that the closer the cumulative distribution curve to the diagonal line is, the more uniform the droplet size distribution is. As indicated in Fig. 9 a–d, for different throat diameters, the cumulative distribution curve of each GLR is above the diagonal, which indicates that the droplet size is concentrated in a smaller size. With an increase in the GLR, the cumulative distribution curve shifts to the upper left of the dashed diagonal line, which suggests that the ratio of the smaller droplets tends to increase. This result is consistent with the above findings that have been analyzed in-depth.

Additionally, as the throat diameter increases, the cumulative distribution curves of the droplets gradually approach from the upper left to the dashed diagonal line. This finding proves that the cumulative distribution consists primarily of smaller droplets and that the distribution pattern of droplets gradually changes from a concentrated distribution to a uniform distribution, and the atomization performance becomes worse. When the throat diameter is small ($D_0 = 1.2$ mm), the variation in the cumulative distribution with the change in the GLR is not obvious. The droplet size is concentrated into a smaller size, and the atomization quality is excellent. For a larger throat diameter ($D_0 = 1.8$ mm), the cumulative distribution evidently moves to the dashed diagonal line with a decrease in the GLR, and the atomization quality deteriorates obviously. Moreover, the effect of the throat diameter on the

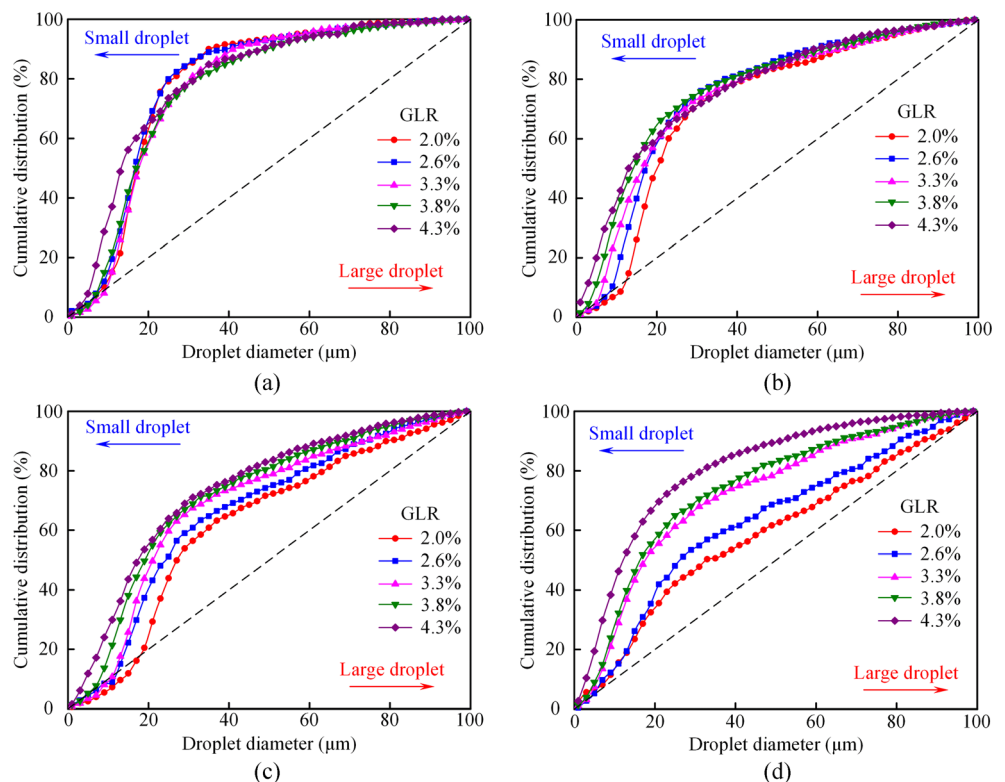
cumulative distribution of droplets is not apparent when the GLR is large, which reveals that, for the NTN, the GLR is the major factor affecting the atomization quality rather than the throat diameter.

3.2.2 Effect of the exit diameter on the droplet size distribution characteristics

To investigate the influence of the exit diameter of the atomizing core on the droplet size distribution characteristics, under various GLR values (2.0%, 2.6%, 3.3%, 3.8%, and 4.3%), the droplet diameter of the NTN with different exit diameters ($D_0 = 1.4$ mm, $L = 3.0$ mm) was measured. Figure 10 shows a comparison of the variation in the droplet counts percent as a function of different exit diameters. As shown, the peak of the droplet size distribution moves to the left with an increase in the GLR from 2.0 to 4.3%, and the counts percent of small size droplets increase, while that of large size droplets decrease. This phenomenon indicates that an increase in the GLR is beneficial for finely atomizing the droplets, and it agrees well with the analysis results in Section 3.2.1.

Furthermore, under the same operating conditions (such as a GLR of 4.3%), the peak appears at 5.4 μm with a value of 14.6% for $D_1 = 2.7$ mm, while the peak and counts percent of the droplet size distribution are 9.5 μm and 12.3% for $D_1 = 3.6$ mm, respectively. With an increase in the exit diameter of the atomizing core, the peak of the droplet size distribution increases obviously, and the ratio of the large droplet increases

Fig. 9 Influence of the throat diameter of the atomizing core on the droplet cumulative distribution at various GLR values. **a** $D_0 = 1.2$ mm. **b** $D_0 = 1.4$ mm. **c** $D_0 = 1.6$ mm and **d** $D_0 = 1.8$ mm



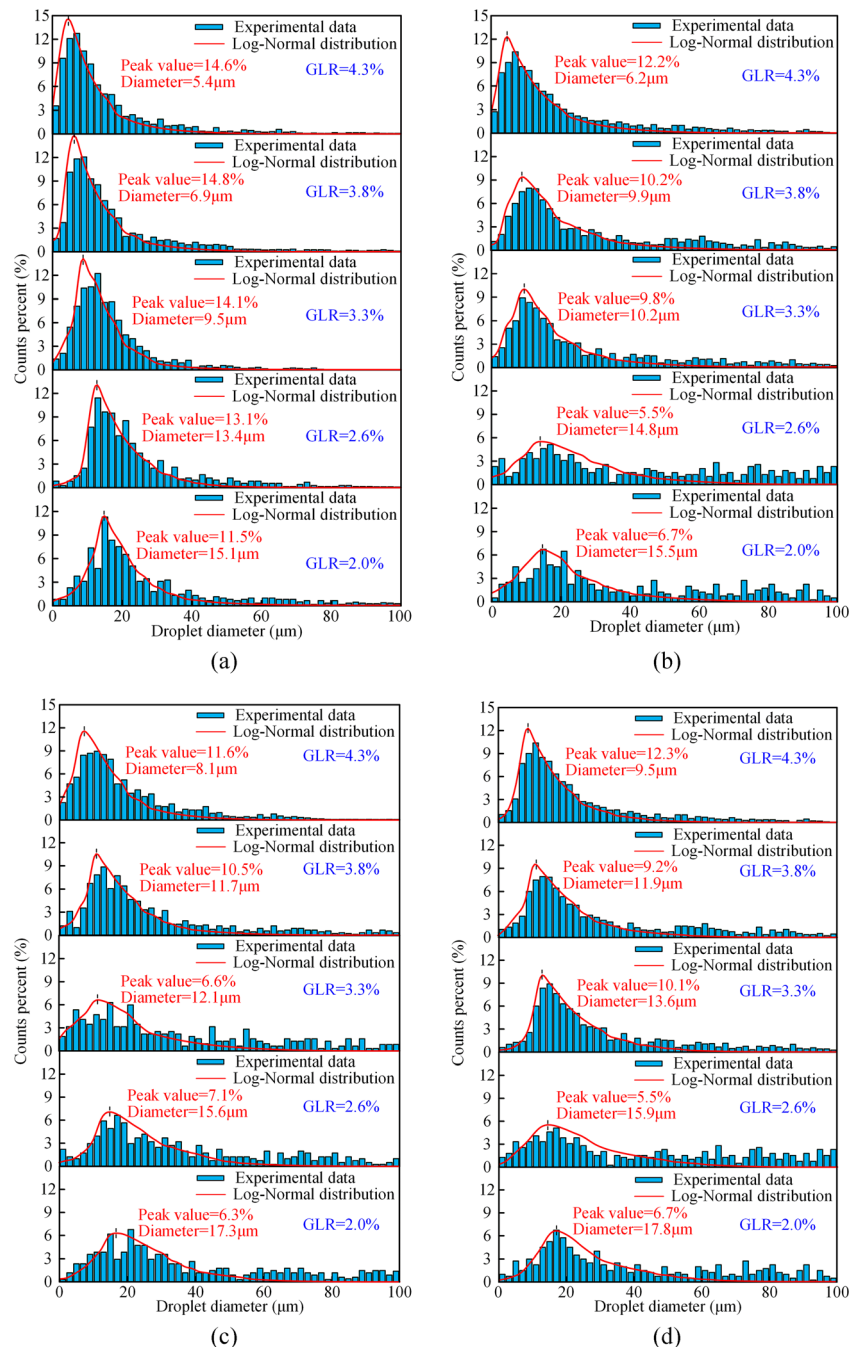
as well as the droplet size distribution becomes discrete. In summary, the atomization behavior shows an obvious deteriorating trend as the exit diameter increases. Cai et al. [37, 38] reported that a decrease in the exit diameter helps increase the velocity both inside and outside the Laval nozzle. Therefore, on the one hand, the reduction in the internal flow velocity inside the nozzle leads to a degradation of the primary atomization performance; on the other hand, a decrease in the outside flow velocity weakens the turbulence around the nozzle outlet, which limits the ability of droplet breakup in the secondary atomization. This results in a deterioration of the

overall atomization performance of the NTN with an increase in the exit diameter of the atomizing core.

Figure 11 illustrates a comparison of the droplet cumulative distribution of the NTN with different atomizing core exit diameters at various GLR values. When the exit diameter is 2.7 mm, for a droplet size of 10 μm , with an increase in the GLR, the cumulative distribution increases from 13.62% (for 2.0%), 18.17% (for 2.6%), 37.89% (for 3.3%), and 48.69% (for 3.8%) to 57.27% (for 4.3%). The cumulative distribution with a droplet size of less than 20 μm is above 50% under these GLR values (2.0%, 2.6%, 3.3%, 3.8%, and 4.3%), and

Fig. 10 Influence of the exit diameter of the atomizing core on the droplet counts percent at various GLR values.

a $D_1 = 2.7$ mm. **b** $D_1 = 3.0$ mm. **c** $D_1 = 3.3$ mm and **d** $D_1 = 3.6$ mm



when the GLR is 4.3%, the cumulative distribution even reaches 80%. However, when the exit diameter is 3.6 mm, the large droplets accounted for nearly half of the total distribution when the GLR increased from 2.3 to 3.6%. This result indicates that excellent atomization performance gradually deteriorates as the exit diameter increases, which is more remarkable under a smaller GLR. This effect is mainly caused by the performance degradation of the primary and secondary atomization of the NTN, as analyzed above. Therefore, it can be concluded that the atomized droplets with a smaller size and a more concentrated distribution are easier to obtain under a higher GLR and smaller exit diameter.

3.2.3 Effect of the liquid channel location on the droplet size distribution characteristics

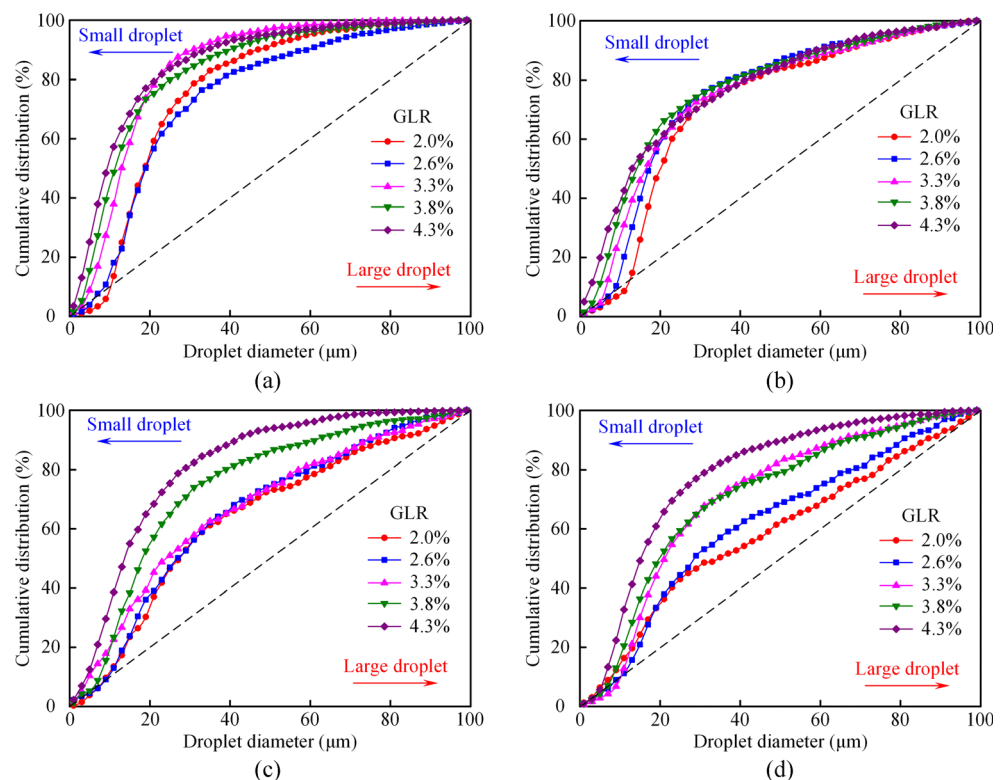
For a better understanding of the influence of the liquid channel location of the atomizing core on the droplet size distribution characteristics, the droplet diameter properties of the NTN at various GLR values were measured and investigated, and the variation in the droplet counts percent as a function of different distances between the liquid channel and atomizing core exit ($D_0 = 1.4$ mm, $D_1 = 3.0$ mm) are shown in Fig. 12. As shown, for four different distances, with a decrease in the GLR from 4.3 to 2.0%, the peak of the droplet size distribution gradually moves to the right and the counts percent of small size droplets decrease obviously. The decrease in the GLR, that is, the reduction in the injection power, leads to a

deterioration of the atomization quality [39–42]. This result agrees well with the analysis results in Section 3.2.1 and validates that the droplet diameter quality of the NTN is obviously affected by increasing GLR.

In addition, for each GLR, the change in the peak of the droplet size distribution is similar. A higher GLR of 4.3% is selected as representative, and the peak appears at 8.7 μm with a value of 14.3% for $L = 2.4$ mm, while the peak and counts percent of droplet size distribution are 10.2 μm and 8.5% for $L = 4.2$ mm, respectively. With an increase in L , the peak of the droplet size distribution first decreases when L is 2.4 to 3.0 mm and then increases when L is 3.0 to 4.2 mm. A superior droplet size distribution is obtained when L is 3.0 mm, which is probably caused by an adequate mixing of the gas-liquid two phases and excellent primary atomization performance [43–45]. This result shows that 3.0 mm is the appropriate distance between the liquid channel and atomizing core exit for improving the droplet atomization performance.

Figure 13 depicts the variation in the droplet cumulative distribution of the NTN with different distances between the liquid channel and atomizing core exit at various GLR values (2.0%, 2.6%, 3.3%, 3.8%, and 4.3%). When the L is 2.4 mm, for a droplet size of 10 μm , with an increase in the GLR, the cumulative distribution increases from 9.08% (for 2.0%), 12.95% (for 2.6%), 13.77% (for 3.3%), and 16.62% (for 3.8%) to 23.24% (for 4.3%). However, the cumulative distribution with a droplet size of less than 20 μm is below 50% under these GLR values, and when the GLR is as high as

Fig. 11 Influence of the exit diameter of the atomizing core on the droplet cumulative distribution at various GLR values. **a** $D_1 = 2.7$ mm. **b** $D_1 = 3.0$ mm. **c** $D_1 = 3.3$ mm and **d** $D_1 = 3.6$ mm

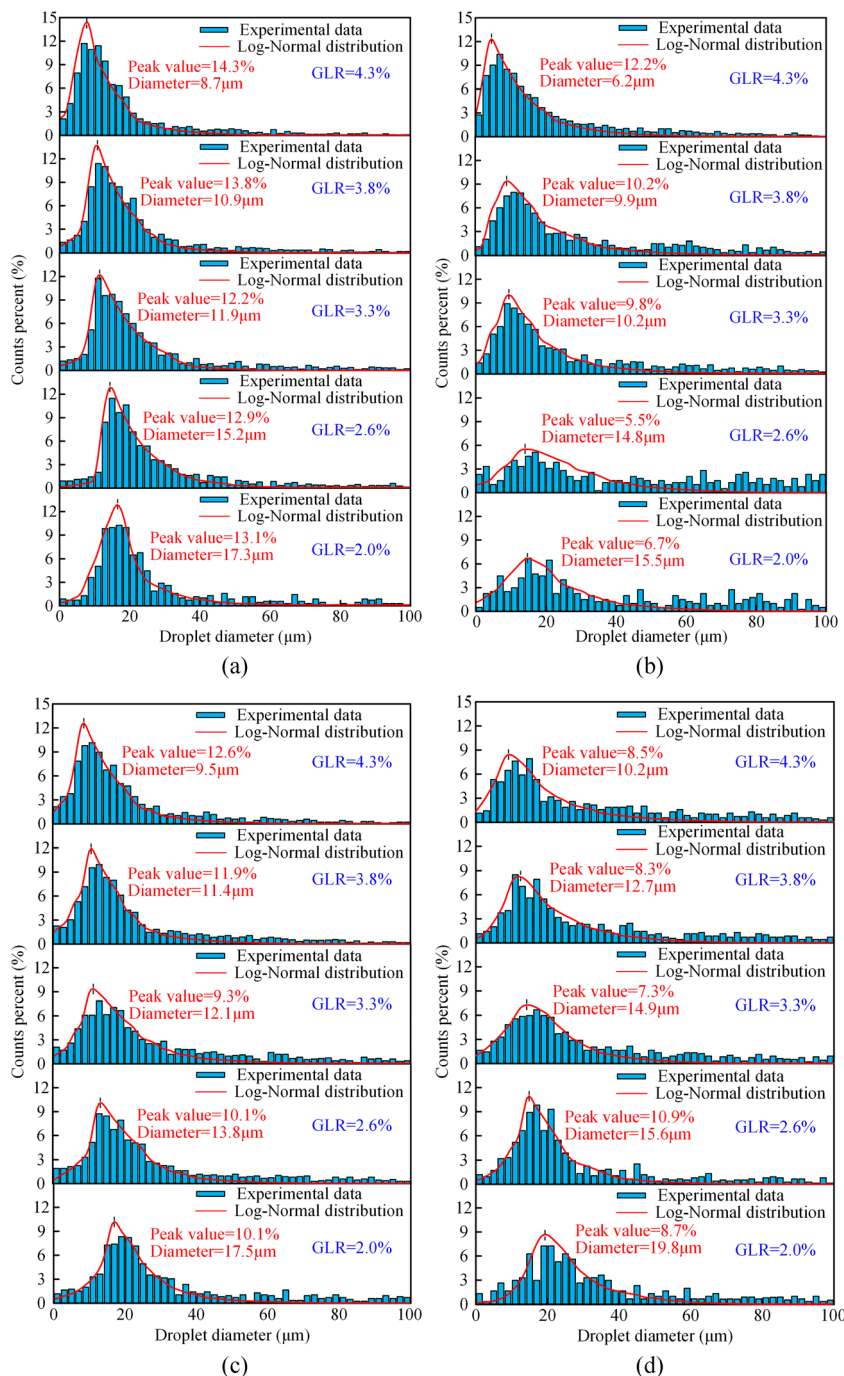


4.3%, the cumulative distribution is only 48.78%. The main reason for this phenomenon is that the location of the liquid channel is closer to the exit of the atomizing core, the interaction between the gas-liquid two phases in the atomizing core is insufficient, which causes the tearing and breakup of a larger droplet to be weak inside the atomizing core, and the primary atomization performance is poor. However, as the L increases, the liquid channel moves toward the throat of the atomizing core, and the small droplets for each GLR increase significantly, as shown in Fig. 13 b–d. This result indicates that the two-

phase fluid is fully mixed inside the atomizing core, the interaction between the gas and liquid is vigorous and sufficient, the tearing and breaking of the droplets is more thorough, and the large-sized droplets are broken into small droplets. The atomization quality is obviously improved.

Furthermore, when the L increases from 3.0 to 4.2 mm, a better droplet cumulative distribution is presented under a higher GLR (3.3%, 3.8%, and 4.3%), while a poor droplet cumulative distribution appears under a lower GLR (2.0% and 2.6%). Previous research has shown that there is an

Fig. 12 Influence of the distance between the liquid channel and atomizing core exit on the droplet counts percent at various GLR values. **a** $L = 2.4$ mm. **b** $L = 3.0$ mm. **c** $L = 3.6$ mm and **d** $L = 4.2$ mm



expansion acceleration process after the gas passes through the throat structure, which leads to an increase in the energy of the gas [46–48]. When L continues to increase, the liquid channel may be located in the acceleration region of the gas energy, which results in a decline in the atomization quality for a smaller GLR due to insufficient energy. Nonetheless, when the atomizing core has a larger GLR, the liquid channel location has less effect on the droplet quality because of the sufficient atomization power.

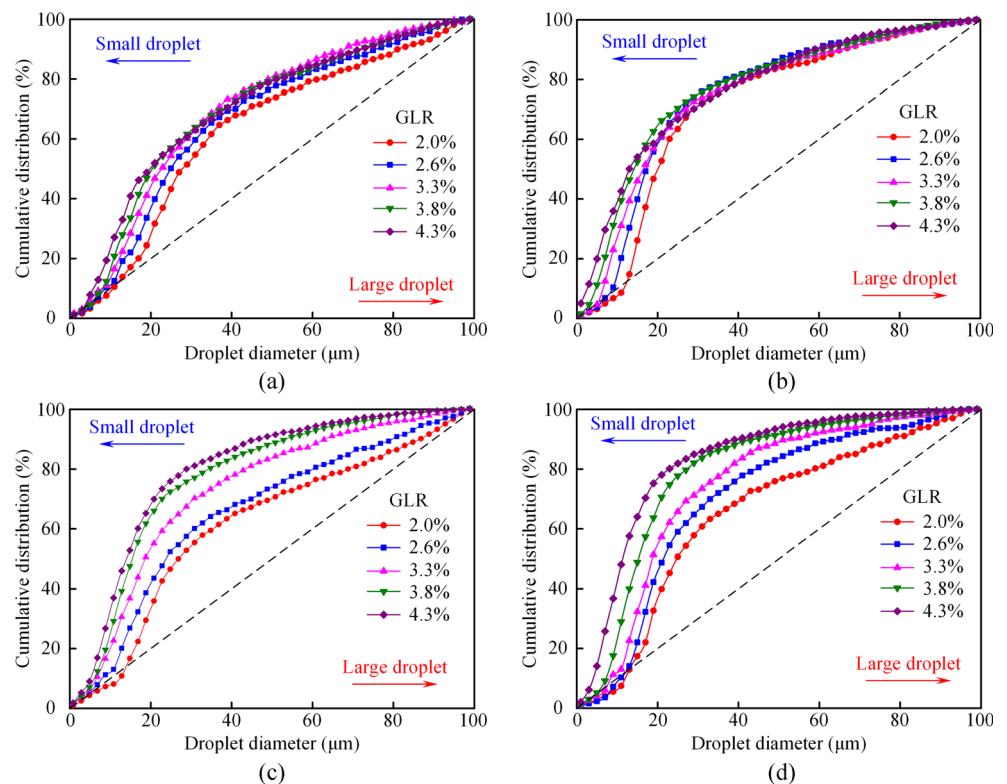
4 Conclusions

To explore the droplet characteristics under the collaborative atomization of a twin-fluid nozzle, the droplet diameter, number concentration, and axial velocity as well as the spray cone angle were measured and obtained under various GLR values, and the spray atomization characteristics of STN and NTN were investigated and compared. Meanwhile, the droplet diameter and size distribution of the twin-fluid nozzles with a new atomizing core were further analyzed, and the investigations were conducted to illustrate the effect of the atomizing core structure on the droplet size distribution characteristics. The conclusions can be summarized as follows:

(1) During the collaborative atomization process of the twin-fluid nozzle, a better gas acceleration performance of the atomizing core and a strong injection power of the higher

- GLR can both enhance the primary atomization and secondary atomization, resulting in the promotion of the spray atomization performance.
- (2) During the collaborative atomization process of the twin-fluid nozzle, a better gas acceleration performance of the atomizing core and a strong injection power of the higher GLR can both enhance the primary atomization and secondary atomization, resulting in the promotion of the spray atomization performance.
 - (3) Because of the more energy provided by a higher GLR at a constant liquid mass flow, the droplet momentum increases, and the viscous force between the liquids is easier to overcome, which leads to an obvious improvement in the atomization characteristics, such as the diameter, number concentration, axial velocity, and spray cone angle.
 - (4) With a larger GLR, the droplet size distribution is less affected by the structural parameters of the NTN atomizing core due to the powerful atomization energy. However, for a smaller GLR, it has a significant effect on the overall droplet diameter and size distribution because of the insufficient atomization power.
 - (5) With the change in the structural parameters of the NTN atomizing core, the droplet cumulative distribution shows different variation trends due to the collaborative atomization behavior. A better cumulative distribution can be obtained with a smaller throat diameter, smaller exit diameter, and moderate distance between the liquid

Fig. 13 Influence of the distance between the liquid channel and atomizing core exit on the droplet cumulative distribution at various GLR values. **a** $L = 2.4$ mm. **b** $L = 3.0$ mm. **c** $L = 3.6$ mm and **d** $L = 4.2$ mm



channel and atomizing core exit. In this study, the throat diameter is 1.2 mm, the exit diameter is 2.7 mm, and the distance is 3.0 mm, which is the appropriate value to choose.

Funding information This work was supported by the Natural Science Foundation of Zhejiang Province (grant number LR18E050003), the National Natural Science Foundation of China (grant numbers 51905481 and 51975523), the Open Foundation of the State Key Laboratory of Fluid Power and Mechatronic Systems (grant number GZKF-201820), the Natural Science Foundation of Hebei Province (grant number E2017203129), and Postdoctoral Preferred Funding Project of Zhejiang Province (grant number zj2019019).

References

- Zhang X, Li C, Jia D, Gao T, Zhang Y, Yang M, Li R, Han Z, Ji H (2019) Spraying parameter optimization and microtopography evaluation in nanofluid minimum quantity lubrication grinding. *Int J Adv Manuf Technol* 103(5–8):2523–2539
- Su Y, Lu Q, Yu T, Liu Z, Zhang C (2019) Machining and environmental effects of electrostatic atomization lubrication in milling operation. *Int J Adv Manuf Technol* 104(5–8):2773–2782
- Mao C, Zhou X, Yin L, Zhang M, Tang K, Zhang J (2016) Investigation of the flow field for a double-outlet nozzle during minimum quantity lubrication grinding. *Int J Adv Manuf Technol* 85(1–4):291–298
- Xu X, Lv T, Luan Z, Zhao Y, Wang M, Hu X (2019) Capillary penetration mechanism and oil mist concentration of Al₂O₃ nanoparticle fluids in electrostatic minimum quantity lubrication (EMQL) milling. *Int J Adv Manuf Technol* 104(5–8):1937–1951
- Poozesh S, Grib S, Renfro M, Marsac P (2018) Near-field dynamics of high-speed spray dryer annular two fluid nozzle: effects of operational conditions and formulations. *Powder Technol* 333:439–448
- Danh V, Jiang L, Akinyemi O (2019) Investigation of water spray characteristics in the near field of a novel swirl burst injector. *Exp Thermal Fluid Sci* 102:376–386
- Zaremba M, Weiß L, Malý M, Wensing M, Jedelský J, Jicha M (2017) Low-pressure twin-fluid atomization: effect of mixing process on spray formation. *Int J Multiphas Flow* 89:277–289
- Luo H, Nishida K, Uchitomi S, Ogata Y, Zhang W, Fujikawa T (2018) Microscopic behavior of spray droplets under flat-wall impinging condition. *Fuel* 219:467–476
- Wang Z, Wen J, Wang J, Dong Q (2014) PDPA investigation on an electrostatically-assisted twin-fluid atomization flow. *Adv Mech Eng* 6:402747
- Luo H, Nishida K, Ogata Y (2019) Evaporation characteristics of fuel adhesion on the wall after spray impingement under different conditions through RIM measurement system. *Fuel* 258:116163
- Fan X, Wang J, Zhao F, Li J, Yang T (2018) Eulerian–Lagrangian method for liquid jet atomization in supersonic crossflow using statistical injection model. *Adv Mech Eng* 10(2):13
- Kim K, Choi Y (2018) Numerical simulation on the generation of ultrasound and formation of water fog in the ultrasonic gas atomizer. *Ultrasonics* 11:002
- Baillet F, Blaisot J, Boisdron G, Dumouchel C (2009) Behaviour of an air-assisted jet submitted to a transverse high-frequency acoustic field. *J Fluid Mech* 640:305–342
- Narayanan S (2013) Atomization in the acoustic field of a Hartmann whistle. *Int J Spray Combust* 5(1):1–24
- Narayanan S, Srinivasan K, Sundararajan T (2013) Acoustic characteristics of external chamfered Hartmann whistles. *Appl Acoust* 74(9):1104–1116
- Ruan C, Xing F, Huang Y, Yu X, Zhang J, Yao Y (2017) The influence of acoustic field induced by HRT on oscillation behavior of a single droplet. *Energies* 10(1):48
- Ficuciello A, Blaisot J, Richard C, Baillet F (2017) Investigation of air-assisted sprays submitted to high frequency transverse acoustic fields: droplet clustering. *Phys Fluids* 29(6):319–321
- Gelfand B (1996) Droplet breakup phenomena in flows with velocity lag. *Prog Energ Combust* 22(3):201–265
- Theofanous T (2011) Aerobreakup of Newtonian and viscoelastic liquids. *Annu Rev Fluid Mech* 43:661–690
- Yang C, Chen B, Jiang W, Gao D, Jin G (2016) Analysis and experiment on atomizing characteristics of supersonic nozzle based on Laval effect. *Trans Chinese Soc Agric Eng* 32(19):57–64
- Mates S, Settles G (2005) A study of liquid metal atomization using close-coupled nozzles, part 1: gas dynamic behavior. *Atom Sprays* 15(1):19–40
- Mates S, Settles G (2005) A study of liquid metal atomization using close-coupled nozzles, part 2: atomization behavior. *Atom Sprays* 15(1):41–60
- Chen B, Gao D, Liang Y, Zhao J, Sun Y (2018) Experimental investigation of atomization and droplet turbulence characteristics of a twin-fluid nozzle with different self-excited vibrating cavity structures. *Exp Thermal Fluid Sci* 99:525–536
- Chen B, Gao DR, Yang C (2017) Atomizing characteristics of twin-fluid impact nozzle based on PDPA. *Trans Chinese Soc Agric Mach* 48(4):362–369
- Bian J, Cao X, Yang W, Guo D, Xiang C (2020) Prediction of supersonic condensation process of methane gas considering real gas effects. *Appl Therm Eng* 164:114508
- Canosa A, Ocana A, Antinolo M, Ballesteros B, Jiménez E, Albaladejo J (2016) Design and testing of temperature tunable de Laval nozzles for applications in gas-phase reaction kinetics. *Exp Fluids* 57(9):152
- Chen B, Gao D, Wu S, Zhao J (2018) Influence of self-excited vibrating cavity structure on droplet diameter characteristics of twin-fluid nozzle. *Chin J Mech Eng* 31(1):73
- Hou D, Jiang W, Zhao W, Bian J, Liu Y, Lai X (2018) Effect of linetype of convergent section on supersonic condensation characteristics of CH₄-CO₂ mixture gas in Laval nozzle. *Chem Eng Process* 133:128–136
- Ochowiak M (2013) The experimental study on the viscosity effect on the discharge coefficient for effervescent atomizers. *Exp Thermal Fluid Sci* 50:187–192
- Kourmatzis A, Lowe A, Masri A (2017) Conditioned analysis of effervescent atomization. *J Energ Eng* 143(5):04017019
- Xia Y, Khezzer L, Alshehhi M, Hardalupas Y (2018) Atomization of impinging opposed water jets interacting with an air jet. *Exp Thermal Fluid Sci* 93:11–22
- Mlkvik M, Stahle P, Schuchmann H, Gaukel V, Jedelsky J, Jicha M (2015) Twin-fluid atomization of viscous liquids: the effect of atomizer construction on breakup process, spray stability and droplet size. *Int J Multiphas Flow* 77:19–31
- Madero J, Axelbaum R (2017) Spray breakup and structure of spray flames for low-volatility wet fuels. *Combust Flame* 180:102–109
- Santolaya J, Garcia J, Calvo E, Cerecedo L (2013) Effects of droplet collision phenomena on the development of pressure swirl sprays. *Int J Multiphas Flow* 56:160–171
- Jia W, Li P, Qiu B, Shi A (2008) Application of phase Doppler particle analyzer in reek spray nozzle's characteristic experiment. *China Rural Water and Hydrop* 2008(9):70–72
- Wittner M, Karbstein H, Gaukel V (2018) Pneumatic atomization: beam-steering correction in laser diffraction measurements of spray droplet size distributions. *Appl Sci-Basel* 8(10):1738

37. Cai Y, Liu Z, Shi Z (2017) Effects of dimensional size and surface roughness on service performance for a micro Laval nozzle. *J Micromech Microeng* 27(5):055001
38. Cai Y, Liu Z, Shi Z, Song Q, Wan Y (2015) Residual surface topology modeling and simulation analysis for micro-machined nozzle. *Int J Precis Eng Man* 16(1):157–162
39. Zeng X, Qiu W, Ji S, Xi F, Qiu L, Zheng Q, Meng S (2019) Optimization and experimental research on process parameters of the softness consolidation abrasive particles. *Int J Adv Manuf Technol* 104(1–4):1017–1026
40. Zeng X, Li J, Ji S, Pan Y, Hang W (2017) Research on machining characteristic of double-layer elastomer in pneumatic wheel method. *Int J Adv Manuf Technol* 92(1–4):1329–1338
41. Zeng X, Li Z, Xi F, Ji S, Qiu L, Shi M, Zheng Q, Qiu W (2019) Material removal characteristic of laser cladding cobalt-based alloy in the photochemical process. *Metals* 9(6):1–13
42. Qiu L, Ji S, Zeng X, Jin M, Li Z, Ge M (2019) Research on partition segment grinding path method of aero-engine blade based on robot group. *IEEE SENS J*. <https://doi.org/10.1109/JSEN.2019.2949250>
43. Piao Z, Xu B, Wang H, Yu X (2019) Rolling contact fatigue behavior of thermal-sprayed coating: a review. *Crit Rev Solid State Mat Sci*. <https://doi.org/10.1080/10408436.2019.1671798>
44. Piao Z, Zhou Z, Xu J, Wang H (2019) Use of X-ray computed tomography to investigate rolling contact cracks in plasma sprayed Fe–Cr–B–Si coating. *Tribol Lett* 67(1):11
45. Ba K, Yu B, Gao Z, Zhu Q, Ma G, Kong X (2019) An improved force-based impedance control method for the HDU of legged robots. *ISA T* 84:187–205
46. Pavlov V, Tunik Y (2012) Detonation combustion of hydrogen in a Laval nozzle under rarefied atmosphere conditions. *Fluid Dynam* 47(5):647–653
47. Matz M, Aumiller M (2014) Practical comparison of cylindrical nozzle and de Laval nozzle for wire arc spraying. *J Therm Spray Techn* 23(8):1470–1477
48. Ba K, Yu B, Zhu Q, Gao Z, Ma G, Jin Z, Kong X (2019) The position-based impedance control combined with compliance-eliminated and feedforward compensation for HDU of legged robot. *J Frankl Inst Eng Appl Math* 356(16):9232–9253

Publisher's note Springer Nature remains neutral with regard to jurisdictional claims in published maps and institutional affiliations.